RESEARCH ARTICLE

NANO · MICRO small
www.small-journal.com

Graphene Derived from Municipal Solid Waste

*Karla J. Silva, Kevin M. Wyss, Carolyn H. Teng, Yi Cheng, Lucas J. Eddy, and James M. Tour**

Dedicated to Prof. PM Ajayan on the occasion of his 62nd birthday

Landfilling is long the most common method of disposal for municipal solid waste (MSW). However, many countries seek to implement different methods of MSW treatment due to the high global warming potential associated with landfilling. Other methods such as recycling and incineration are either limited to only a fraction of generated MSW or still produce large greenhouse gas emissions, thereby providing an unsustainable disposal method. Here, the production of graphene from treated MSW is reported that including treated wood waste, using flash Joule heating. Results indicated a 71%–83% reduction in global warming potential compared to traditional disposal methods at a net cost of −$282 of MSW, presuming the graphene is sold at just 5% of its current market value to offset the cost of the flash Joule heating process.

1. Introduction

Increased municipal solid waste (MSW) generation has long been attributed to population and urbanization growth.[1] As more MSW is generated, MSW management has become a major concern for many municipalities. In its most recent studies, the Environmental Protection Agency of the United States (EPA) estimated that out of the estimated 292 million tons of MSW produced by the United States in 2018, ≈50% was managed through landfilling, suggesting landfilling to be the most common form of MSW management.[2] Though landfilling is typically the least expensive method of MSW disposal, it has been associated with significant land usage and volume uptake, but more concerningly toxic leachate release (**Figure 1**).[3–6] Landfill leachate is typically composed of components including diverse organics, inorganics including toxic heavy metals, and xenobiotics such as polychlorinated aromatic hydrocarbons.[4–6] Landfill leachate represents a significant pollution threat to waterways, and though various regulations have improved landfill construction to slow leachates from contaminating waterways, sustainable leachate management is difficult to achieve due to leachate compositions varying across landfills.[7–9] Landfilling also releases large amounts of methane (CH_4) and carbon dioxide (CO_2).[10] Many countries are therefore implementing alternative strategies to landfilling.

Other common methods of mitigating MSW in developed countries include recycling and incineration. However, recycling is expensive, requires extensive sorting by humans, typically results in a downcycled product, and is limited to a fraction of MSW content.[2,11–14] Incineration of MSW has been shown to be an economically feasible option that allows for volume reduction while limiting CH_4 emissions when compared to landfilling. However, incineration has been known to emit greater amounts of CO_2, and it also emits nitride oxides, which have a larger global warming potential (GWP) than does CH_4. Dioxins and other organic pollutants with ranging toxicity are released upon incineration (Figure 1).[15–17] With global MSW production expected to increase by as much as 45% by 2050, it is imperative to find methods to both reduce the amount of landfilled MSW and to provide an alternative management method.[18]

Flash Joule heating (FJH) is a method that has previously been used to convert various carbon-rich feedstocks into graphene.[19–21] By applying a high-voltage electrical discharge through a minimally conductive sample, heat is rapidly generated, facilitating rapid carbon bond dissociation. These carbon bonds reform to produce the thermodynamically most favored sp^2-hybridized graphene lattice. Rather than forming ordered, AB-stacked graphene in which electron-rich areas overlap on top of electron-deficient areas in the graphene sheet below, resulting in compact interlayer spacing, the rapid cooling rate results in rotationally disoriented graphene sheets that are referred to as turbostratic graphene because the graphene sheets do not have sufficient time to orient themselves.[19] This is particularly desirable since the rotational disorientation of the sheets

K. J. Silva, K. M. Wyss, C. H. Teng, Y. Cheng, J. M. Tour
Department of Chemistry
Rice University
6100 Main Street, Houston, TX 77005, USA
E-mail: tour@rice.edu
L. J. Eddy, J. M. Tour
Department of Physics
Rice University
6100 Main Street, Houston, TX 77005, USA
J. M. Tour
Department of Materials Science and NanoEngineering
Smalley-Curl Institute
Nanocarbon Center and the Rice Advanced Materials Institute
Rice University
6100 Main Street, Houston, TX 77005, USA

The ORCID identification number(s) for the author(s) of this article can be found under https://doi.org/10.1002/smll.202311021

DOI: 10.1002/smll.202311021

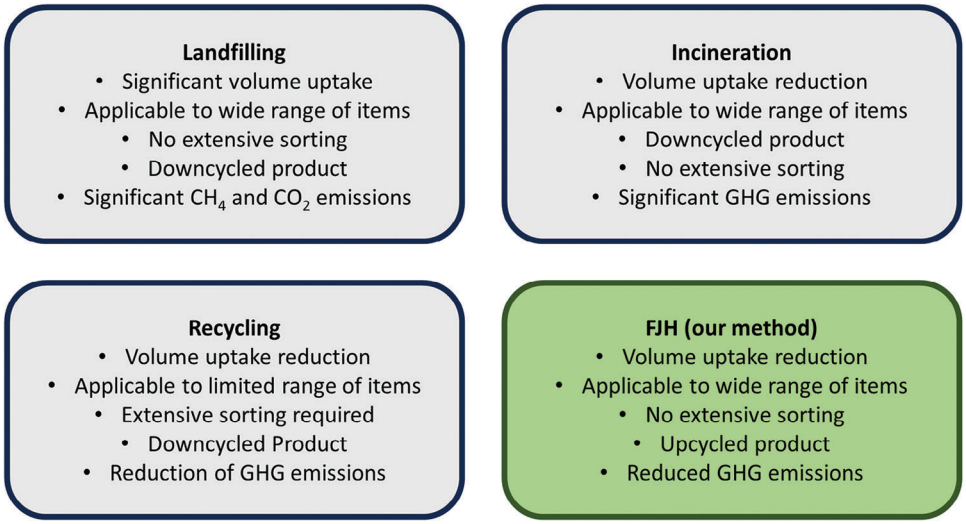

Figure 1. A scheme comparing common MSW management methods and FJH.

facilitates greater exfoliation efficiency rendering their more facile dispersion in composites.[19] Graphene has many demonstrated applications ranging from composite reinforcement to lubricant enhancement.[22,23] Since major components of MSW, including food waste and waste plastics, are typically carbon-rich, FJH is a plausible method to convert MSW into graphene (Figure 1).[2] Here, we report the use of FJH to convert treated MSW (MSWT) into turbostratic graphene. Part of MSW is treated waste wood (WWT) that comes from construction waste and tree or plant trimmings. This WWT acts as a suitable conductive additive to decrease the electrical resistance in other MSW, rendering the mixed material suitable for FJH.

2. Results and Discussion

2.1. FJH Process

Since FJH reactions involve electric current, the reactant must be somewhat electrically conductive, but not too conductive such that there are no resistive hotspots and so that Joule heating can occur.[19] Using a mixture of MSW commercially pretreated at 316 °C (MSWT, 67%) along with commercially pretreated waste wood (WWT, 33%) as a conductive additive, a resistance of 620 Ω was achieved. These pretreatments are routine in many municipalities to lower the water content and the toxicity of MSW. The mixtures of MSWT and WWT were subjected to alternating current (AC) FJH, which entails passing an electrical current through the sample itself, resulting in a lowering of the resistance to 4–5 Ω, which is an optimal resistance for direct current (DC) FJH.[19] A 100 V discharge through the mixture resulted in a current measurement of 210 A with a corresponding maximum temperature of ≈2550 °C (**Figure** 2a,b). Additional FJH reactions were required to produce sample homogeneity and optimal graphene conversion. 160 and 235 V discharges resulted in currents of 670 and 1450 A along with associated temperatures of 2750 °C and 1460 °C, respectively (Figures 2c,d). The final discharge at 235 V likely resulted in a lower maximum temperature than previous discharges due to the lower resistance encountered in the sample. Although typically an increased voltage discharge would result in higher heat generation, the sample is at such a low resistance (≈0.67 ohms) that resistive heating is not facilitated. The total duration including one AC discharge and the 3 DC discharges was 7 s. A final resistance of 0.10 Ω was recorded. Previous work indicates temperatures nearing 2800 °C are sufficient to convert amorphous carbon into turbostratically stacked graphene.[19] A mass yield of 45% was recorded; however, this is solely calculated from the total weight out divided by the total weight in. Many of the elements were non-carbon (H and O) in the starting materials, so the actual yield of graphene-based solely on carbon was determined using elemental analysis and calculated to be 57%. Graphene yield could likely be enhanced by optimizing sample resistance, increasing discharge voltage, and varying the duration of FJH.[19]

2.2. Characterization of Graphitic Product

The feedstocks and FJH reaction products were characterized using Raman spectroscopy. Average Raman spectra corresponding to WWT and MSWT show the presence of a *D* band occurring at 1350 cm^{-1} and a G band occurring at 1582 cm^{-1}. The *D* band only arises when defects are present in the lattice structure, whereas the G band arises through the vibration of sp^2 carbon atoms.[24,25] Based on the Raman spectra, the WWT and MSWT are amorphous carbon. In the average Raman spectrum of the MSWT/WWT graphene product, a small *D* band is observed along with the G band and the clear emergence of a 2D band at 2700 cm^{-1} (**Figure** 3a). The average D/G intensity ratio of 0.46 and average 2D/G intensity ratio of 0.97 suggest high-quality graphene production since the low-intensity *D* band suggests there is little disorder in the MSWT/WWT graphene. The high-resolution Raman spectrum of the MSWT/WWT graphene shows the presence of TS_1 and TS_2 peaks occurring at 1875 and 2025 cm^{-1} establishing the graphene to be turbostratic, and the missing M peak at 1750 cm^{-1} indicates no detectable AB-stacking

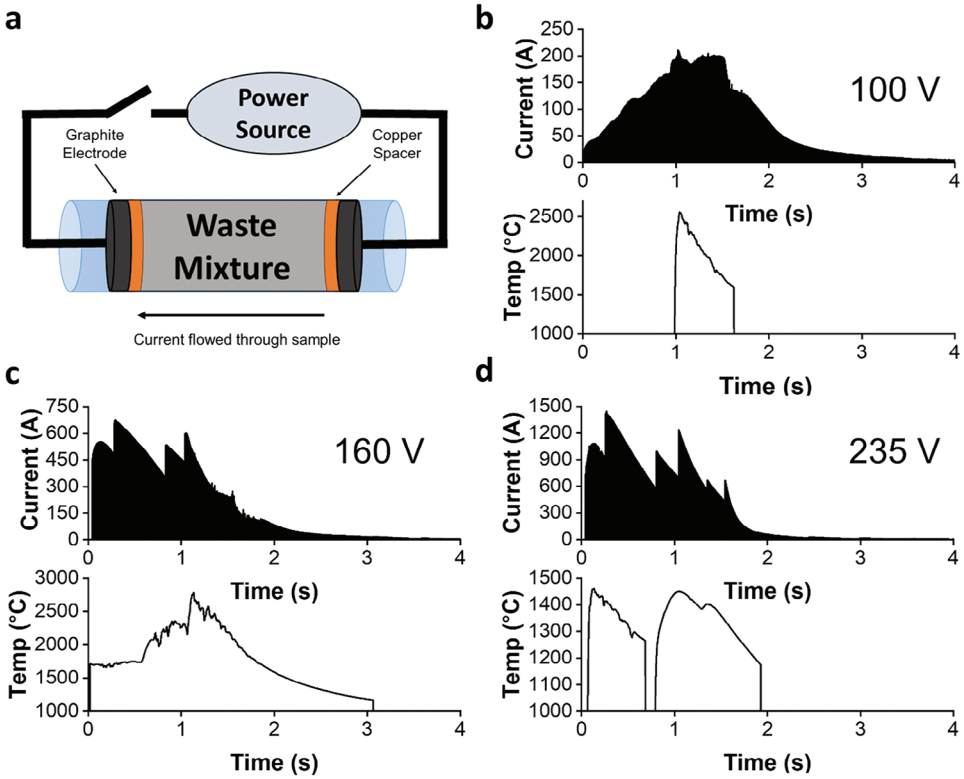

Figure 2. FJH schematic, current along with temperature profiles during various electrical discharges of the FJH of MSWT/WWT mixture a) FJH scheme b–d) Current measured during FJH with associated temperature measurements during the FJH of MSWT/WWT mixture at 100, 160, and 235 V discharge, respectively. In Figure 2d, a rapid decrease in temperature is observed. This is attributed to the temporary misalignment of the pyrometer used to obtain temperature readings because of the vibrations of the system during FJH.

(Figure 3b).[26] The M peak at 1750 cm^{-1} results from the strong coupling between graphene sheets in AB-stacked graphene.[26]

Powder X-ray diffraction (XRD) analysis was used to study the bulk characteristics of the materials. The XRD spectrum of WWT is further evidence that WWT is amorphous carbon while the XRD spectrum of MSWT also indicates the presence of silicon carbides and silicon oxides. In the MSWT/WWT graphene, it is observed that many of the impurities are volatilized out of the sample and the main impurity is SiC (Figure 3c). The broadening of the (002) peak encountered on average at 26.1° can be traced to an average lattice spacing of 0.340 nm using Bragg's Law.[27] The rotational disorder results in the increased interlayer spacing from 0.335 nm that is observed in AB-stacked graphite to the observed 0.340 nm average lattice spacing in the turbostratic graphene product.

Elemental analysis was conducted along with X-ray photoelectron spectroscopy (XPS) to determine the elemental composition of the bulk material, and its surface composition, respectively. Elemental analysis suggests the composition of WWT to be 83.4% C, and 0.2% H, while XPS survey scans indicate WWT to have 11.4% O. MSWT has a composition of 62.2% C and 6.77% H according to elemental analysis and an O content of 18.4%, Si content of 8.3%, and trace amounts of Ca, Zn, K, and Cl by XPS elemental scans. FJH of the MSWT/WWT mixture resulted in an increased C content of 87.7% and an overall H content of 1.8% while the O content decreased to 8.8% (Figure 3d).

XPS also confirms the expulsion of impurities through FJH since a notable decrease in the intensity of the Si peak is observed in the graphene product when compared to MSWT (Figure 3e). Si presence decreased from an average of 8.3% in MSWT to an average of 0.41% in the MSWT/WWT graphene by XPS analysis. Si has a boiling point of 2355 °C, whereas carbon boiling would not occur until 4827 °C. XPS survey scans also indicate trace amounts of metals such as Ca, Zn, and K remain in the MSWT/WWT graphene but at <0.2%. High-resolution scans of C*1s* suggest the presence of C—C bonding and also suggest the main impurity to be SiC through the presence of Si—C bonding. Tables S1 and S2 (Supporting Information) contain the XPS analyses of MSWT and MSWT/WWT graphene, respectively. These results were used to determine the Si content of the materials.

Thermogravimetric analysis (TGA) in air was used to further study the bulk character of the graphene product. MSWT displays signs of thermal degradation at 330 to 455 °C with ≈10% inorganic content. WWT degrades at 465 to 550 °C with <3% inorganics. After undergoing FJH, the product graphene displays increased thermal stability with gradual degradation at ≈525 to 700 °C with ≈18% inorganic content, assuredly some coming from inorganic oxide formation during the TGA analysis (Figure 3f). From XRD and XPS analyses of the residual TGA mass upon heating to 800 °C, the components that remain after heating to 800 °C are silicon carbides and silicon oxides (Figures S1 and S2, Supporting Information).

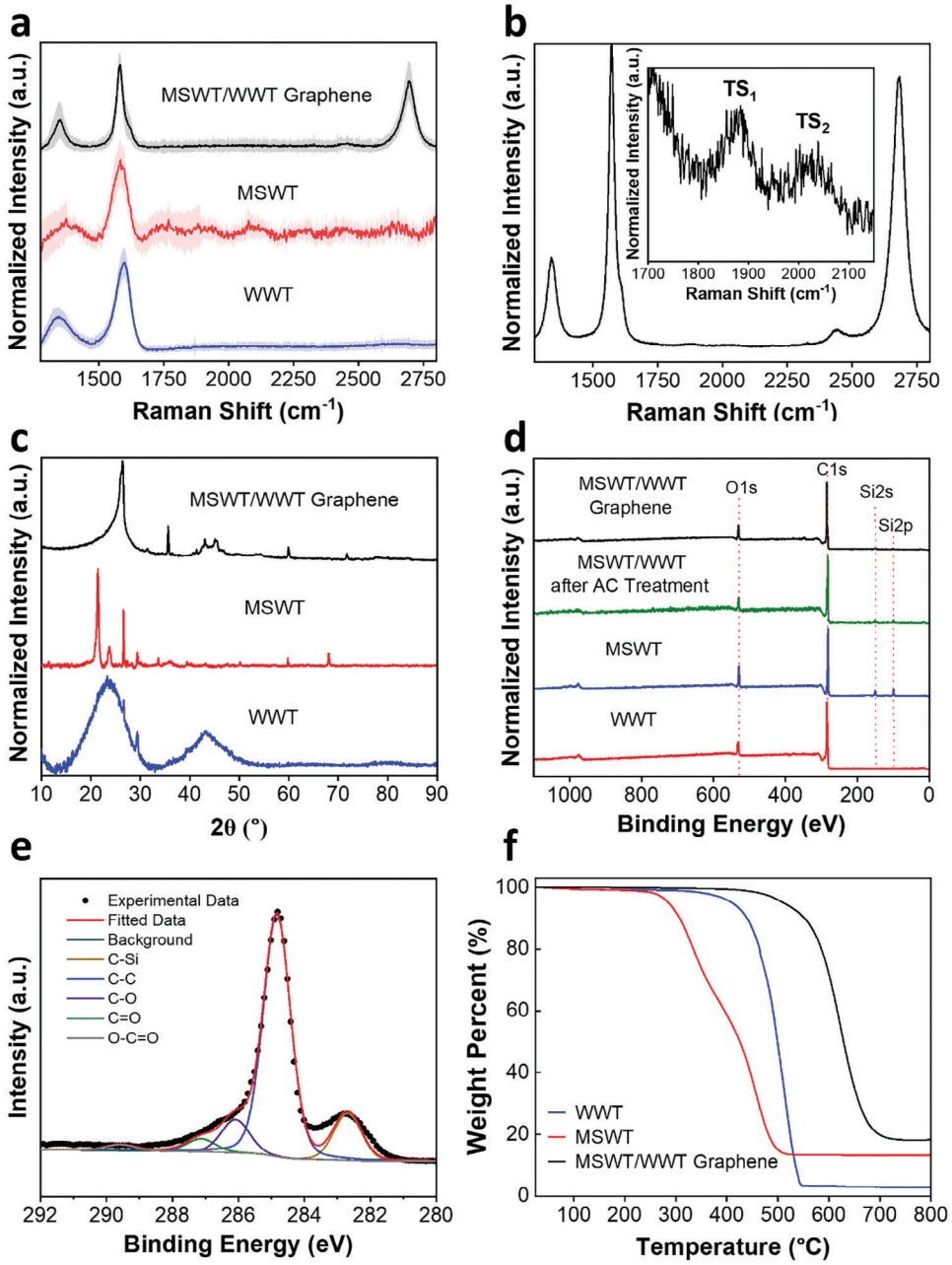

Figure 3. Characterization of starting materials and the graphene product. a) Average Raman spectra of starting MSWT, WWT, and MSWT/WWT-derived graphene. (200 individual spectra over a 1 mm^2 area for WWT and graphene and 200 spectra over a 0.5 mm^2 area for MSWT) with standard deviations represented by shaded regions. b) High-resolution Raman spectra indicating the presence of TS_1 and TS_2 peaks from turbostratic stacking of MSWT/WWT graphene. c) Bulk XRD spectrums of starting materials and the MSWT/WWT-derived graphene. d) XPS survey scans of starting materials, MSWT/WWT mixture after one AC treatment, and the final graphene. e) High-resolution scans of C*1s* of the graphene f) TGA (air, 11 °C min^{-1}) of starting materials and graphene suggesting increased thermal stability of the graphene compared to starting MSWT and WWT materials.

2.3. Electron Microscopy

Electron microscopy was employed to study morphological changes after FJH. Scanning electron microscopy (SEM) displayed the stacked morphology of the graphene that is shown at various magnifications in **Figure** 4a, in strong contrast to the dense structures encountered in WWT and MSWT (Figures S3 and S4, Supporting Information). High-resolution transmission electron microscopy (HR-TEM) micrographs depict lattice fringes indicating the high crystallinity of the graphene (Figure 4b,c). Fast Fourier transform of a selected region depicts polycrystalline graphitic material while an interlayer spacing of 0.349 nm is observed, once again suggesting the graphene product has an increased interlayer spacing compared to AB-stacking (Figures S5 and S6, Supporting Information).

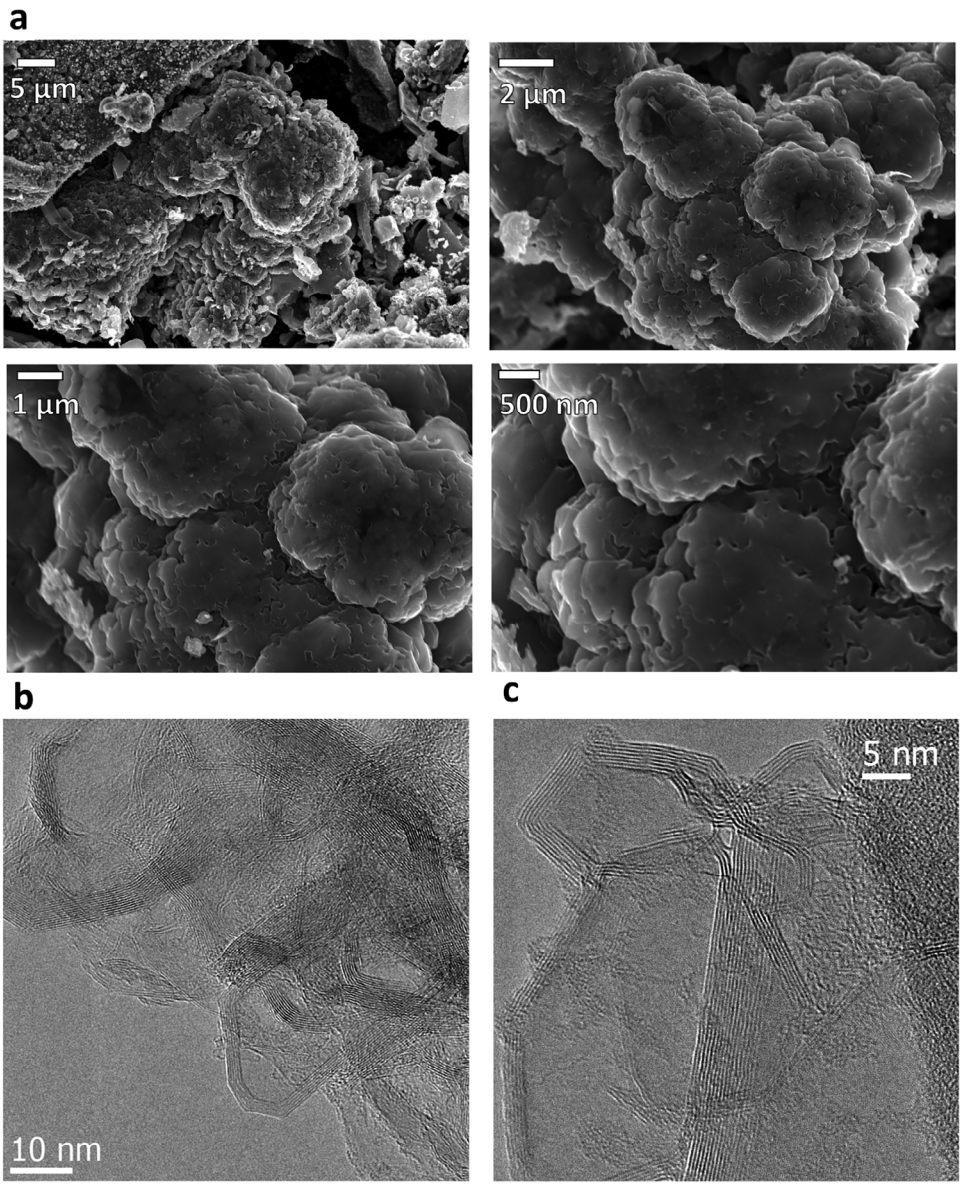

Figure 4. Electron microscopy of MSWT/WWT graphene. a) SEM images depicting sheet-like morphology in MSWT/WWT graphene at various magnifications with associated scale bars. b,c) TEM micrograph of MSWT/WWT graphene highlighting lattice fringes.

2.4. Surface Area Analysis and Dispersion Testing

Brunauer–Emmett–Teller (BET) surface area analysis reveals WWT to have a surface area of 117 $m^2\ g^{-1}$, while MSWT has a much lower surface area of 1.8 $m^2\ g^{-1}$. Once the MSWT/WWT mixture undergoes FJH, the resulting surface area of the MSWT/WWT graphene is 5.6 $m^2\ g^{-1}$ (**Figure 5a**). Pore size is significantly decreased by the FJH of the MSWT/WWT mixture when compared to WWT, yet the pore size is comparable to that encountered in MSWT (Figures S7–S9, Supporting Information).

The dispersibility of the MSWT/WWT graphene was tested in 1% Pluronic-127, a surfactant, against flash graphene derived from metallurgical coke (MC-FG) (Figure 5b). At low concentrations, the MSWT/WWT graphene product displayed similar dispersibility to that of MC-FG, while at increased loadings, the dispersibility of MC-FG is greater. The lower dispersibility of the graphene product derived from MSWT/WWT could likely be attributed to the low surface area.

2.5. Gas Analysis of Volatiles Evolved During FJH Process

The volatile gases produced in the FJH of the MSWT/WWT mixture were captured and analyzed using gas chromatography (Figures S10–S12 and Tables S3–S5, Supporting Information). Volatiles evolved during the FJH process were determined to include hydrogen, carbon monoxide, and trace amounts of methane, carbon dioxide, and other hydrocarbons. The average ratio of CO_2 to CO was calculated to be 0.66. Using this, the

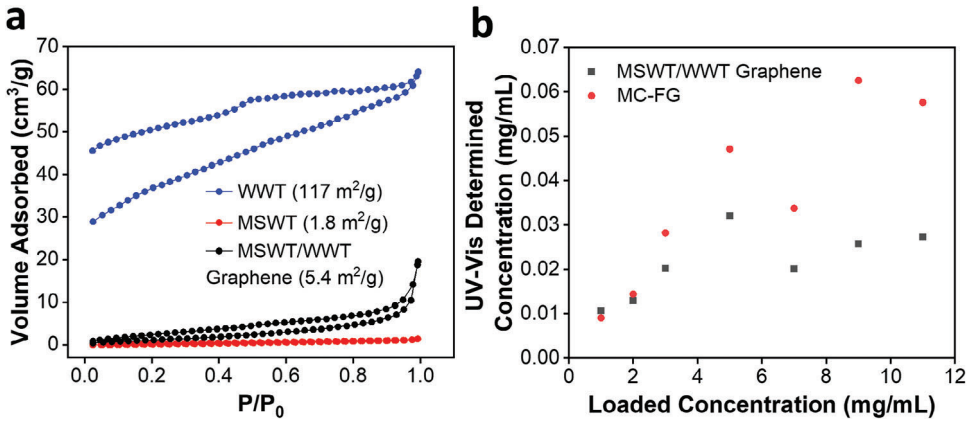

Figure 5. BET analysis and dispersion in 1% pluronic F-127 solution of MSWT/WWT-derived graphene and MC-FG. a) BET analysis of feedstocks and resulting graphene. b) Dispersion of MSWT/WWT graphene and MC-FG in pluronic F-127.

calculated CO_2 evolved during FJH would be 0.635 kg per tonne of reaction mixture assuming linear scaling. On average, hydrogen (H_2) content was found to be 28% of the volatiles evolved and ≈22% of available H_2 was recovered as H_2. H_2 (≈10 kg) could be produced by one tonne of reaction mixture. Recent work suggests the tunability of FJH to produce H_2 gas from waste plastic, indicating further work could provide even greater yields of H_2.[28] H_2 gas and CO production also provide a pathway to fuel production, thereby providing yet another attractive product from FJH MSW.

2.6. Life Cycle Assessment and Technoeconomic Analysis

A life cycle assessment (LCA, **Figure 6**) was used to determine the 100-year global warming potential (GWP_{100}) of the FJH process when compared to common methods of MSW management such as biogas capture with flaring, landfilling, and incineration (scope discussed on pp Figures S12–S15, Supporting Information). Recycling was not included since the range of items that can be recycled is substantially limited. Results indicate that FJH lowers greenhouse gas emissions (Figures S13–S15 and Tables S6–S7, Supporting Information). FJH can decrease GWP_{100} by up to 83% when compared to landfilling with a gas capture and flare system (LF+GC) and decrease by 71% when compared to incineration (Table S8, Supporting Information). This makes FJH a potentially much more environmentally friendly method of MSW disposal. The net cost of FJH reacting one ton of MSW would be −$282 presuming the sale of only the graphene by-product at only 5% ($3000 ton^{-1}), which would be a "worst case scenario," of the present market value of $60 000 ton^{-1}. Incineration, on the other hand, would result in a net cost of $48 ton^{-1} presuming the electricity generated is sold and the toxic ash by-product is treated. Incineration would result in the disposal of ash into landfills whereas graphene, the byproduct of FJH, could be used in other applications such as composite reinforcement, lubrication enhancement, or even sodium ion batteries due to its increased layer spacing.[22,23,29] Therefore, FJH provides a method that not only lowers GWP_{100} but is both economically favorable and reduces materials destined for landfills.

3. Conclusion

We demonstrate the feasibility of using FJH to convert MSWT and WWT into turbostratic graphene, using two waste products that are normally sent to landfills. Through FJH we provide a potential alternative method to landfilling for MSW management. FJH provides not only a 71%–83% GWP_{100} reduction but an overall net cost of −$282 per 1000 kg of MSW, making it highly economically attractive.

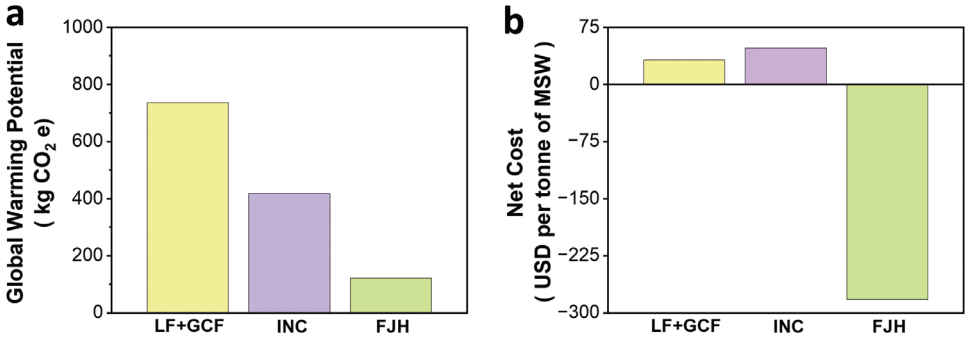

Figure 6. Life cycle assessment of common MSW management compared to FJH a) GWP associated with common MSW management methods such as landfilling with a gas capture and flare system (LF+GCF) and incineration (INC) compared to FJH b) Technoeconomic analysis impacts associated with landfilling with a LF+GCF and INC as compared to FJH, in US dollars (USD).

4. Experimental Section

Feedstocks: MSW was provided by Midwest Custom Solutions, LLC which they dried at 120 °C for ≈15 min followed by torrefaction at 316 °C for 90 min, a thermochemical process that decreases the water and volatile content of the biomass, improving some of its fuel properties.[30] The waste was composed of 50% cardboard and paper and 50% food and plastic waste. The WWT was provided by Liberty Ashes, Inc., and its commercial treatment was not disclosed.[31]

FJH of MSWT/WWT Mixture: Batches of MSWT (0.67 g) and WWT (0.33 g), a total of 1.00 g, were loaded between two pieces of copper woold rolled into cylinders, referred to as spacers, within quartz tubes (16 mm inner diameter).[19] Fritted graphite spacers were used as electrodes to facilitate outgassing. The samples were compressed until a resistance of ≈620 Ω was achieved and were then subjected to alternating current FJH (1–3 s) resulting in 4–5 Ω resistance. This entails passing an electrical current through the sample. The sample was then subjected to FJH using direct current at 10%, 20%, and 50% 1 kHz duty cycles at 1 s, 0.5 s, and 5 s durations, respectively, with a rated capacity of 624 mF at 100, 160, and 235 V discharges.[19]

Characterization: Feedstocks and FJH products were each ground using mortar and pestle and then characterized using Raman Spectroscopy (Renishaw inVia Raman microscope, 5 mW 532 nm laser, 50× objective lens), bulk-powder XRD (Rigaku SmartLab II, zero background holder, 7° min^{-1} with 0.05° step size), thermogravimetric analysis, (under air at an 11 °C min^{-1} heating rate), and BET surface area analysis (Quantachrome Autosorb-iQ3-MP/Kr BET, N analysis gas, with 6 h degas at 120 °C under high vacuum). The morphology of the FJH MSWT/WWT product graphene product was studied through scanning electron microscopy (FEI Helios NanoLab 660 Dual Beam System, 15 keV) and that of the starting materials was also studied (FEI ESEM 15, 1.5 keV). XPS analysis was carried out using a PHI Quantera SXM Scanning X-Ray Microprobe (5×10^{-9} Torr operating pressure, with 0.1/140 eV step size and pass energy for survey scans, with 0.1/26 eV step size and pass energy for high-resolution elemental scans). Dispersion analysis was carried out using UV–vis spectroscopy (Shimadzu UV–vis 3600i Plus at 660 nm). Gases evolved during FJH were characterized using gas chromatography with an Agilent 8890 GC system equipped with an Agilent HP-5 ms low-bleed column (30 m, 0.25 mm internal diameter, 0.25 µm film) with helium as the carrier gas for liquid and headspace sampling. A tandem Agilent 5977B mass selective detector was used for headspace gas analysis.

Supporting Information

Supporting Information is available from the Wiley Online Library or from the author.

Acknowledgements

The funding for the research was provided by the U.S. Army Corps of Engineers, ERDC (W912HZ-21-2-0050), and the Air Force Office of Scientific Research (FA9550-22-1-0526). The authors acknowledge the Shared Equipment Authority (SEA) at Rice University for the characterization instrumentation. The authors thank Midwest Solutions LLC for MSWT and Liberty Ashes Inc. for WWT. K.J.S designed the experiments and conducted the characterizations. K.M.W. contributed to the experimental design and characterization. C.T., Y.C., and L.E. contributed to experimentation. K.J.S and J.M.T. wrote and edited the manuscript. All aspects of the research were overseen by J.M.T. All authors discussed the results and commented on the manuscript.

Conflict of Interest

Rice University owns intellectual property on technologies here. That has been licensed to a company in which JMT is a shareholder, though not an officer, director, or employee. Conflicts of interest are managed through regular disclosures to the Office of Sponsored Programs and Research Compliance.

Data Availability Statement

The data that support the findings of this study are available in the supplementary material of this article.

Keywords

flash Joule heating, global warming potential, municipal solid waste, sustainable, waste wood

Received: November 28, 2023
Revised: April 22, 2024
Published online:

[1] A. Kumar, E. Singh, R. Mishra, S. L. Lo, S. Kumar, *Energy* **2023**, *275*, 127471.
[2] U. S. EPA, *National Overview: Facts and Figures on Materials, Wastes and Recycling*, https://www.epa.gov/facts-and-figures-about-materials-waste-and-recycling/national-overview-facts-and-figures-materials (accessed: November 2023).
[3] A. D. Read, P. Phillips, G. Robinson, *Resour. Conserv. Recycl.* **1997**, *20*, 183.
[4] R. Gonzalez-Valencia, F. Magana-Rodriguez, J. Cristóbal, F. Thalasso, *Waste Manag* **2016**, *55*, 299.
[5] H. I. Abdel-Shafy, A. M. Ibrahim, A. M. Al-Sulaiman, R. A. Okasha, *Ain Sham. Eng. J.* **2023**, *15*, 102293.
[6] S. A. Al Raisi, *EJGEO* **2022**, *3*, 1.
[7] M. T. El-Saadony, A. M. Saad, N. A. El-Wafai, H. E. Abou-Aly, H. M. Salem, S. M. Soliman, T. A. Abd El-Mageed, A. S. Elrys, S. Selim, M. E. Abd El-Hack, S. Kappachery, K. A. El-Tarabily, S. F. AbuQamar, *Environ. Technol. Innov.* **2023**, *31*, 103150.
[8] E. R. Bandala, A. Liu, B. Wijesiri, A. B. Zeidman, A. Goonetilleke, *Environ. Pollut.* **2021**, *291*, 118133.
[9] M. A. Kamaruddin, M. S. Yusoff, H. A. Aziz, Y.-T. Hung, *Appl Water Sci* **2015**, *5*, 113.
[10] K. Spokas, J. Bogner, J. P. Chanton, M. Morcet, C. Aran, C. Graff, Y. M.-L. Golvan, I. Hebe, *Waste Manage.* **2006**, *26*, 516.
[11] B. G. Mwanza, in *Recent Developments in Plastic Recycling. Composites Science and Technology*, (Eds: J. Parameswaranpillai, S. Mavinkere Rangappa, A. Gulihonnehalli Rajkumar, S. Siengchin), Springer, Singapore, **2021**.
[12] J. P. Lange, *ACS Sustainable Chem. Eng.* **2021**, *9*, 15722.
[13] N. Kajiwara, H. Matsukami, G. Malarvannan, P. Chakraborty, A. Covaci, H. Takigami, *Chemosphere* **2022**, *289*, 133179.
[14] Y. Guo, X. Xia, J. Ruan, Y. Wang, J. Zhang, G. A. LeBlanc, L. An, *Sci. Total Environ.* **2022**, *838*, 156038.
[15] Z. Fu, S. Lin, H. Tian, Y. Hao, B. Wu, S. Liu, L. Luo, X. Bai, Z. Guo, Y. Lv, *Sci. Total Environ.* **2022**, *826*, 154212.
[16] C. Li, L. Yang, J. Wu, Y. Yang, Y. Li, Q. Zhang, Y. Sun, D. Li, M. Shi, G. Liu, *J. Hazard. Mater* **2022**, *428*, 128220.
[17] B. Liu, Z. Han, X. Liang, *Atmos. Pollut. Res.* **2023**, *14*, 101842.
[18] A. Maalouf, A. Mavropoulos, *Waste Manag. Res* **2023**, *41*, 936.
[19] D. X. Luong, K. V. Bets, W. A. Algozeeb, M. G. Stanford, C. Kittrell, W. Chen, R. V. Salvatierra, M. Ren, E. A. McHugh, P. A. Advincula, Z. Wang, M. Bhatt, H. Guo, V. Mancevski, R. Shahsavari, B. I. Yakobson, J. M. Tour, *Nature* **2020**, *577*, 647.
[20] P. A. Advincula, D. X. Luong, W. Chen, S. Raghuraman, R. Shahsavari, J. M. Tour, *Carbon* **2021**, *178*, 649.

[21] W. A. Algozeeb, P. E. Savas, D. X. Luong, W. Chen, C. Kittrell, M. Bhat, R. Shahsavari, J. M. Tour, *ACS Nano* **2020**, *14*, 15595.
[22] P. A. Advincula, W. Meng, L. J. Eddy, J. L. Beckham, I. R. Siqueira, D. X. Luong, W. Chen, M. Pasquali, S. Nagarajaiah, J. M. Tour, *Macromol. Mater. Eng.* **2023**, *308*, 2200640.
[23] P. A. Advincula, V. Granja, K. M. Wyss, W. A. Algozeeb, W. Chen, J. L. Beckham, D. X. Luong, C. F. Higgs, J. M. Tour, *Carbon* **2023**, *203*, 876.
[24] M. J. Allen, V. C. Tung, R. B. Kaner, *Chem. Rev.* **2010**, *110*, 132.
[25] Z. Ni, Y. Wang, T. Yu, Z. Shen, *Nano Res.* **2008**, *1*, 273.
[26] R. Rao, R. Podila, R. Tsuchikawa, J. Katoch, D. Tishler, A. M. Rao, M. Ishigami, *ACS Nano* **2011**, *5*, 1594.
[27] C. G. Pope, *J. Chem. Educ.* **1997**, *74*, 129.
[28] K. M. Wyss, K. J. Silva, K. V. Bets, W. A. Algozeeb, C. Kittrell, C. H. Teng, C. H. Choi, W. Chen, J. L. Beckham, B. I. Yakobson, J. M. Tour, *Adv. Mater.*, *35*, 2306763.
[29] Y. Wen, K. He, Y. Zhu, F. Han, Y. Xu, I. Matsuda, Y. Ishii, J. Cumings, C. Wang, *Nat. Commun.* **2014**, *5*, 4033.
[30] *Midwest Custom Solutions*, http://www.midwestcustomsolutions.com/ (accessed: November 2023).
[31] Liberty Ashes Inc., https://libertyashes.com/contact (accessed: November 2023).